Original Article

Quantitative FDG PET/CT may help risk-stratify early-stage non-small cell lung cancer patients at risk for recurrence following anatomic resection

Stephanie Harmon[1], Christopher W. Seder[2], Song Chen[1,3], Anne Traynor[1], Robert Jeraj[1], Justin D. Blasberg[4]

[1]Department of Medical Physics, University of Wisconsin, Madison, WI, USA; [2]Department of Thoracic and Cardiovascular Surgery, Rush University Medical Center, Chicago, IL, USA; [3]Department of Nuclear Medicine, The 1st Hospital of China Medical University, Shenyang 110016, China; [4]Department of Surgery, Yale University, New Haven, CT, USA

Contributions: (I) Conception and design: All authors; (II) Administrative support: R Jeraj; (III) Provision of study materials or patients: None; (IV) Collection and assembly of data: S Harmon, R Jeraj, JD Blasberg; (V) Data analysis and interpretation: All authors; (VI) Manuscript writing: All authors; (VII) Final approval of manuscript: All authors.

Correspondence to: Justin D. Blasberg, MD. 330 Cedar Street, BB 205, New Haven, CT 06510, USA. Email: justin.blasberg@yale.edu.

Background: Preoperative identification of non-small cell lung cancer (NSCLC) patients at risk for disease recurrence has proven unreliable. The extraction of quantitative metrics from imaging based on tumor intensity and texture may enhanced disease characterization. This study evaluated tumor-specific ^{18}F-fluorodeoxyglucose (^{18}F-FDG) positron emission tomography/computerized tomography (PET/CT) uptake patterns and their association with disease recurrence in early-stage NSCLC.

Methods: Sixty-four stage I/II NSCLC patients who underwent anatomic resection between 2001 and 2014 were examined. Pathologically or radiographic confirmed disease recurrence within 5 years of resection comprised the study group. Quantitative imaging metrics were extracted within the primary tumor volume. Squamous cell carcinoma (SCC) (N=27) and adenocarcinoma (AC) (N=41) patients were compared using a Wilcoxon signed-rank test. Associations between imaging and clinical variables with 5-year disease-free survival (DFS) and overall survival (OS) were evaluated by Cox proportional-hazards regression.

Results: Clinical and pathologic characteristics were similar between recurrence (N=34) and patients achieving 5-year DFS (N=30). Standardized uptake value $(SUV)_{max}$ and SUV_{mean} varied significantly by histology, with SCC demonstrating higher uptake intensity and heterogeneity patterns. Entropy-grey-level co-occurrence matrix (GLCM) was a significant univariate predictor of DFS (HR =0.72, P=0.04) and OS (HR =0.65, P=0.007) independent of histology. Texture features showed higher predictive ability for DFS in SCC than AC. Pathologic node status and staging classification were the strongest clinical predictors of DFS, independent of histology.

Conclusions: Several imaging metrics correlate with increased risk for disease recurrence in early-stage NSCLC. The predictive ability of imaging was strongest when patients are stratified by histology. The incorporation of ^{18}F-FDG PET/CT texture features with preoperative risk factors and tumor characteristics may improve identification of high-risk patients.

Keywords: Positron emission tomography (PET); quantitative imaging; early-stage non-small cell lung cancer (early-stage NSCLC); surgical resection; clinical outcome

Submitted Jan 14, 2019. Accepted for publication Apr 03, 2019.
doi: 10.21037/jtd.2019.04.46
View this article at: http://dx.doi.org/10.21037/jtd.2019.04.46

Introduction

Non-small cell lung cancer (NSCLC) remains the number one cause of cancer-associated mortality in the world (1). Patients with early-stage disease (stages I and II) are at higher risk for recurrence compared to other solid organ malignancies of similar stage (2,3). Accurate preoperative staging has a significant impact on surgical outcome, and the incorporation of ^{18}F-fluorodeoxyglucose (^{18}F-FDG) positron emission tomography/computerized tomography (PET/CT) imaging has been integral to define NSCLC subgroups best managed by primary resection. Despite these advancements, including NCCN guidelines that recommend routine use of ^{18}F-FDG PET/CT imaging, 5-year survival for stage I and II NSCLC is only 80–85% and 50%, respectively (4).

Risk-stratification utilizing quantitative PET/CT has demonstrated prognostic significance, particularly in advanced stages of NSCLC, identifying elevated standardized uptake value $(SUV)_{max}$ as a marker for reduced 5-year survival and metabolic tumor volume (MTV) as a marker for decreased survival (5-7). However, commonly used SUV_{max} has not been identified as independent predictors of overall survival (OS) in early stage (I/II) patients (8,9). FDG uptake varies by histologic subtype, confounding the ability for imaging metrics to predict risk for recurrence. For example, differences in SUV_{max} for adenocarcinoma (AC) and squamous cell carcinoma (SCC) have been reported (8,10,11), with notably higher SUV uptake in SCC lesions reflecting a high proliferative index of this cell type (12).

Recently there have been efforts to assess the prognostic significance of FDG heterogeneity within a tumor (13). These higher-order quantitative PET features correlate with several prognostic factors, including survival, risk for recurrence, and resistance to chemotherapy in advanced disease (14,15). Several works have evaluated the prognostic ability of radiomics features in various stages and treatments of lung cancer, including early stage NSCLC (16,17). Complementary work has shown variation in heterogeneity features across NSCLC subtypes (18) and that clustering of radiomics-based features from FDG PET/CT can distinguish AC from SCC tumors (19).

The purpose of this study is to test the ability of quantitative metrics, including texture-based metrics describing heterogeneity, in ^{18}F-FDG PET/CT imaging to predict recurrence following surgical resection of early-stage NSCLC. We further aim to assess the impact of histology-specific FDG PET/CT patterns on correlation to outcome.

Methods

Patient population

This retrospective case-controlled study examined NSCLC resections performed at a single university medical center between 2001 and 2014. The use of STS data for eligible patients was approved by the institutional Internal Review Board. All patients with a new primary diagnosis of NSCLC and preoperative ^{18}F-FDG PET/CT PET imaging that underwent anatomic lung resection for Stage I and II disease (7th edition AJCC/UCII staging system) were evaluated. To ensure quantitative accuracy of this analysis, additional imaging exclusions were applied. A complete list of study inclusion and exclusion criteria are listed (*Table 1*).

Preoperative clinic and inpatient medical records were reviewed to obtain baseline characteristics. Date of death was confirmed from the social security death index, including patients who were lost to clinical follow-up. As standard practice, endobronchial ultrasound-guided fine needle aspiration (EBUS-FNA) and mediastinoscopy are selectively used in this patient population, as clinically indicated. The type of resection performed was based on patient and tumor characteristics, as well as surgeon judgment. Patients are followed with physical exam and non-contrast CT scan every 6 months for the first 2 years, then yearly for life.

Disease recurrence in ipsilateral hemithorax, mediastinum, or a distant site was evaluated within 5 years of resection and determined by either biopsy proven NSCLC or radiographic evidence of disease without a contralateral lung lesion if biopsy was not feasible. In cases where only radiographic data was available, the designation of recurrence, rather than a new primary lung cancer, was based on consensus evaluation at a multi-disciplinary lung tumor board. Controls were defined as patients without disease recurrence and 5-year follow-up who otherwise met inclusion criteria.

Image acquisition and analysis

PET imaging was acquired on one of GE Advance (N=26), GE Discovery LS (N=28), and GE Discovery STE (N=20) scanners (Waukesha, WI, USA). Patients were injected with 10 mCi (range, 9–20 mCi) of ^{18}F-FDG and scanned

Table 1 Patient selection criteria

Inclusion criteria	Exclusion criteria
Clinicopathologic considerations	Clinicopathologic considerations
1. Pathologic stage I or II NSCLC	1. Wedge resection
2. Surgical procedures performed with intent to cure	2. Stage IIIA disease or greater
3. Performance of lobectomy or pneumonectomy	3. Treatment with neoadjuvant chemotherapy or chemoradiation therapy
4. Performance of mediastinal lymph node sampling or dissection	4. The presence of synchronous lung masses
5. Follow-up clinic and imaging data for 5 years postoperatively	5. Lost to follow-up without retrievable records or from which recurrence data could not be determined
	6. Adenocarcinoma *in situ* or more than one tumor in the specimen
	7. Recurrence within 3 months of resection
Imaging considerations	Imaging considerations
1. PET/CT scans performed at the study institution	1. Tumors less than 2 cm
2. Surgical procedures performed within 90 days of imaging study	2. Greater than 90 days between imaging and surgical procedure
3. Imaging performed on one of three dedicated clinical scanners	3. Use of outside or non-dedicated clinical scanner

NSCLC, non-small cell lung cancer; PET/CT, positron emission tomography/computerized tomography.

60 min (±9.2 min) post-injection. All scans were performed to allow acquisition of seven to eight bed positions to cover skull to mid-thigh. After reconstruction, images were normalized to the body mass SUV. Following PERCIST recommendations, normal reference tissue values in a 3-cm-diameter region of interest in the liver to evaluate image quality across the three scanners (20). Acquisition and reconstruction parameters were as follows: Advance (2 min/bp; 3D-ITER reconstruction with 28 iterations, 2 subsets, 3 mm post-filter for final grid size 128×128×205 of 4.3×4.3×4.25 mm^3), Discovery LS (3 min/bp; OSEM reconstruction with 28 iterations, 2 subsets, 3 mm post-filter for final grid size 128×128×205 of 3.9×3.9×4.25 mm^3), Discovery STE (3 min/bp; OSEM reconstruction with 14 iterations, 2 subsets, 5 mm post-filter for final grid size 128×128×311 of 5.5×5.5×3.27 mm^3). Comparison of liver uptake can be found in *Figure S1*, no significant differences in liver uptake was found across the three scanners.

Tumors were automatically segmented on reconstructed PET scans using an institutional algorithm (21). After segmentation, tumor regions of interest (ROIs) were reviewed and manually adjusted if necessary, by a staff nuclear medicine physician. MTV was reported for each patient. All quantitative analyses and feature extraction were performed in MATLAB (MathWorks 2016) (*Table 2*). SUV metrics were calculated over the entire tumor volume, including metrics describing tracer uptake avidity (20). Additionally, three texture-based metrics representing local heterogeneity derived from the grey-level co-occurrence matrix (GLCM) were extracted (22,23). These metrics have shown prognostic potential in prior works (17) and variability due to image acquisition has been characterized. The methodology for 3D voxel-based feature extraction follows the works of Galavis *et al.* (24,25) and other published works (26), as shown in *Figure 1*. SUV metrics are quantized into a number of gray tones for analysis, in this case 256 grey levels, by resampling to the maximum uptake within the ROI (i.e., relative discretization) (25). Next, local neighbors surrounding each voxel contained within the lesion ROI, called a patch, are identified. These patches are defined for XY, XZ, and YZ planes of 5×5 neighbors (i.e., 2 voxel distance) surrounding each voxel within the ROI (26). Texture values are then calculated in each of the planes, averaged for each voxel, and finally averaged across the entire ROI.

Statistical analysis

Wilcoxon's rank sum test was performed to investigate differences in SUV metrics across various pathologic characteristics. Spearman's correlation was performed to investigate the correlation of imaging metrics with

Table 2 Quantitative metrics extracted from lesion ROIs on PET images. Radiomics-based metrics described are second-order metrics from gray-level co-occurrence matrix (GLCM) (13)

Metric	Description
MTV	Volume of ROI
SUV_{max}	Maximum uptake within tumor ROI
SUV_{peak}	1 cm sphere surrounding SUV_{max}
SUV_{mean}	Mean of all uptake values within tumor ROI
TLG	Product of SUV_{mean} and ROI volume
SUV_{stdev}	Standard deviation of uptake values within tumor ROI
Homogeneity	Measure of closeness of elements along the diagonal of GLCM, inversely correlated with Entropy-GLCM
Entropy-GLCM	Measure of randomness in GLCM, thought to provide measure of heterogeneity
Dissimilarity	Measure of variation in pairs of GLCM

ROI, region of interest; PET, positron emission tomography; MTV, metabolic tumor volume; SUV, standardized uptake value; TLG, total lesion glycolysis.

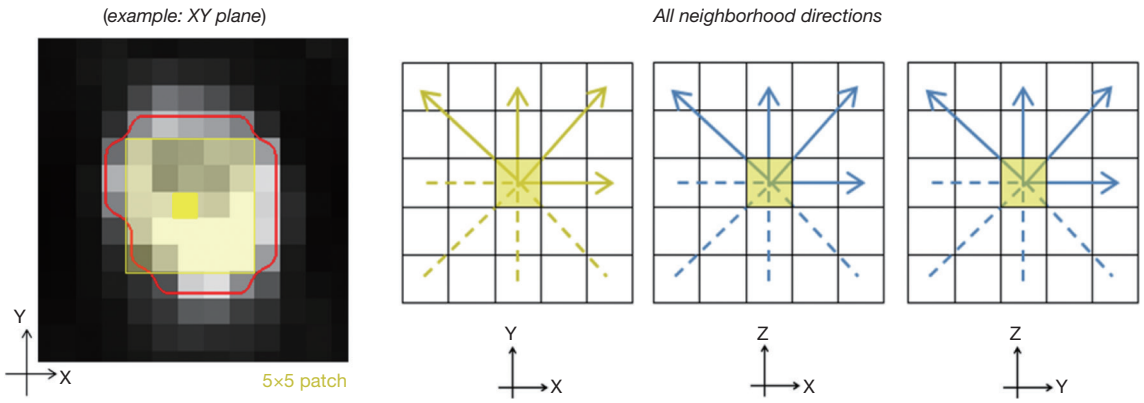

Figure 1 In voxel-based extraction of texture features, neighborhoods are built around a single voxel in regional patches (example 5×5 patches on left). This is computed for XY, XZ, and YZ planes surrounding each voxel. Four directions are considered for each plane.

pathological tumor size and MTV. The primary endpoint was 5-year disease-free survival (DFS), measured from the date of surgical resection to the date of first evidence of tumor recurrence, including locoregional recurrence, distant metastasis, or death. Univariate and multivariate Cox proportional hazard regression analyses were conducted to evaluate associations between clinical and imaging metrics with clinical outcomes (DFS and OS). A multivariate Cox proportional hazard model was created utilizing forward selection, considering univariate predictors of level P<0.2, and backward selection using Bayesian information criteria. The Kaplan-Meier method was used to estimate DFS and OS survival, and compared between groups using the log-rank test. Statistical analysis was performed with R version 3.1.1 (R, The R Foundation). Significance was determined at the 0.05 level and all tests were two-sided.

Results

Sixty-four patients met clinical and imaging criteria for inclusion in this study. The median time between preoperative imaging and surgical resection was 23 days (range, 2–84 days). Thirty-four patients demonstrated recurrent disease within 5 years of resection, with a median DFS interval of 14.9 months (range, 3.6–57.6 months). Patient characteristics and associations with clinical outcomes are listed in *Table 3*. No differences in DFS across clinical stage, pathological tumor stage, or histology

Table 3 Clinical patient characteristics and associations with disease-free and overall survival from Cox proportional hazards regression

Patient characteristics	Category	Number	DFS (N_{events}=34)		OS (N_{events}=26)	
			HR (95% CI)	P value	HR (95% CI)	P value
Age (years)	Mean [range]	69.2 [48–88]	1.06 (0.76–1.47)	0.74	1.06 (0.72–1.55)	0.78
Sex	M	32	Ref	–		
	F	32	0.91 (0.91–1.78)	0.77	1.13 (0.52–2.45)	0.75
Smoking history	Never	3	Ref	–		
	Former	59	0.85 (0.2–3.58)	0.83		
	Current	2	4.8 (0.64–32)	0.13		
Pack years	Mean [range]	38.8 [2–100]	1.07 (0.77–1.49)	0.68	1.28 (0.87–1.89)	0.21
Clinical stage	IA	34	Ref	–		
	IB	14	0.54 (0.2–1.46)	0.23	0.22 (0.05–0.96)	0.04
	IIA	10	1.22 (0.49–3.06)	0.67	1.01 (0.37–2.75)	0.98
	IIB	6	1.25 (0.43–3.68)	0.68	0.55 (0.13–2.45)	0.44
Pathological size	Mean (median)	3.88 (3.05)	1.06 (0.76–1.47)	0.74	0.90 (0.61–1.35)	0.62
Pathological node status	pN0	54	Ref	–		
	pN1	10	3.24 (1.49–7.02)	0.003	4.16 (1.70–11)	0.002
Pre-Op mediastinal staging	No	34	Ref	–		
	Yes	30	2.06 (1.04–4.06)	0.04	2.04 (0.93–4.47)	0.08
Histology	Adenocarcinoma	33	Ref	–		
	Squamous cell carcinoma	26	1.04 (0.51–2.11)	0.92	0.80 (0.36–1.79)	0.58
	Mixed	5	1.33 (0.39–4.54)	0.65	0.38 (0.05–2.92)	0.36
Tumor grade	Well	8	Ref	–		
	Mod	45	3.12 (0.74–13)	0.12	0.93 (0.32–2.72)	0.89
	Poor	11	3.55 (0.74–17)	0.11	0.93 (0.23–3.73)	0.92
Adjuvant chemotherapy	No	52	Ref	–		
	Yes	12	2.49 (1.18–5.23)	0.02	3.04 (1.33–6.96)	0.01
History of hypertension	No	27	Ref	–		
	Yes	37	2.81 (1.31–6.03)	0.008	2.74 (1.13–6.67)	0.03
History of diabetes	No	52	Ref	–		
	Yes	12	0.89 (0.37–2.16)	0.8	0.87 (0.32–2.33)	0.78
DLCO	Mean (median)	76.6 (75.0)	0.63 (0.43–0.92)	0.02	0.55 (0.35–0.87)	0.01
Hemoglobin	Mean (median)	12.8 (12.9)	0.74 (0.52–1.04)	0.08	0.80 (0.54–1.18)	0.26
Creatinine	Mean (median)	0.9 (1.0)	0.70 (0.47–1.04)	0.08	0.87 (0.59–1.27)	0.46
Recurrence location	Local	10	–		–	
	Contralateral	14				
	Distant	10				
Extent of surgery	Lobectomy	63	–		–	
	Pneumonectomy	1				

DLCO, diffusing capacity of the lungs for carbon monoxide.

Table 4 Histology-specific associations with imaging metrics

Metric	AC (N=33), median (SD)	SCC (N=26), median (SD)	P value
MTV	12.8 (25.7)	15.4 (55.1)	0.26
SUV_{max}	8.79 (5.59)	17.0 (7.05)	0.002
SUV_{peak}	5.08 (4.66)	12.69 (5.40)	0.001
SUV_{mean}	3.73 (2.48)	7.05 (2.92)	0.0007
TLG	41.9 (167.6)	67.6 (481)	0.05
Homogeneity	0.015 (0.0003)	0.01 (0.0005)	0.03
Entropy-GLCM	4.24 (0.01)	4.23 (0.02)	0.01
Dissimilarity	39.1 (3.3)	39.5 (3.28)	0.7

MTV, metabolic tumor volume; SUV, standardized uptake value; TLG, total lesion glycolysis; GLCM, grey-level co-occurrence matrix; AC, adenocarcinoma; SCC, squamous cell carcinoma.

were noted. Patients with pathologic node-positive, pN1, disease demonstrated shortened DFS compared to pN(–) (HR =3.24, 95% CI, 1.49–7.02, P=0.003). Patient-specific clinical factors such as history of hypertension and decreased diffusing capacity of the lungs for carbon monoxide (DLCO) were also significantly associated with non-favorable DFS interval. At the time of data collection, 26 of 64 patients had expired. Pathological node status remained the most significant clinical factor, where pN1 disease was significantly associated with shorter survival interval (HR =4.16, 95% CI, 1.70–11, P=0.002).

Quantitative imaging characteristics

Tumors of larger pathological dimension exhibited higher TLG (P=0.86, P<0.001), while Homogeneity and Dissimilarity were inversely associated with tumor size. Using Spearman's correlation, first-order features, such as SUV_{max}, exhibited stronger correlations to tumor size (P>0.5) than texture features (*Table S1*). No significant difference in tumor volume was noted between histologies (P=0.26, *Table 4*). However, all standard SUV metrics and two radiomics-based metrics were significantly different between AC and SCC patients. SCC tumors had higher metrics compared to AC tumors, with the exception of Entropy-GLCM, which was higher in AC (P=0.01).

Entropy-GLCM was the only imaging metric to demonstrate a significant relationship with DFS (*Table 5*). In a multivariate model combining clinical and imaging features (*Table S2*), Entropy-GLCM remained significant (HR =0.65, 95% CI, 0.49–0.87, P=0.004), combining with hemoglobin levels (HR =0.76, 95% CI, 0.61–0.94, P=0.01), DLCO (HR =0.95, 95% CI, 0.93–0.98, P=0.005), history of hypertension (HR =2.83, 95% CI, 1.29–6.22, P=0.01), and tumor grade (HR =8.9, 95% CI, 1.9–41, P=0.005).

Similar to DFS, no standard SUV metrics were associated with OS, though Entropy-GLCM and Homogeneity showed significant associations (*Table 5*). In a multivariate model (*Table S2*), Entropy-GLCM remained an independent predictor of OS (HR =0.60, 95% CI, 0.45–0.81, P=0.0007) along with DLCO (HR =0.96, 95% CI, 0.94–0.99, P=0.005), history of hypertension (HR = 2.97, 95% CI, 1.17–7.52, P=0.02), and use of adjuvant chemotherapy (HR =4.79, 95% CI, 1.9–12, P=0.09).

Impact of histology-specific imaging characteristics on outcome

AC and SCC patients were evaluated separately to identify imaging characteristics associated with DFS for each subgroup (*Table 6*). In SCC patients, radiomics-based metrics (Homogeneity, Entropy-GLCM, and Dissimilarity) were significant predictors of DFS. No radiomics-based imaging characteristics were independent predictors for AC patients. However, SUV_{mean} and TLG showed significant association with DFS. Patients were classified based on histology and histology-specific imaging correlates (Dissimilarity for SCC, SUV_{mean} for AC) using median values reported in *Table 6* for dichotomizing patients. Significant differences in DFS were noted for each group (log-rank P<0.001) when imaging correlates were included in the model (*Figure 2*). The low number of observed

Table 5 Imaging associations with disease-free and overall survival from Cox proportional hazards regression

Metric	DFS (N_{events}=34)		OS (N_{events}=26)	
	HR (95% CI)	P value	HR (95% CI)	P value
MTV	1.06 (0.79–1.41)	0.71	0.91 (0.61–1.35)	0.63
SUV_{max}	1.31 (0.89–1.93)	0.18	0.84 (0.52–1.36)	0.48
SUV_{peak}	1.32 (0.89–1.93)	0.16	0.84 (0.53–1.35)	0.47
SUV_{mean}	1.38 (0.94–2.03)	0.10	0.81 (0.49–1.34)	0.41
TLG	1.10 (0.83–1.46)	0.50	0.89 (0.59–1.32)	0.55
Homogeneity	1.35 (0.97–1.86)	0.07	1.45 (1.05–2.01)	0.03
Entropy-GLCM	0.72 (0.52–0.98)	0.04	0.65 (0.48–0.89)	0.007
Dissimilarity	1.19 (0.87–1.64)	0.28	1.38 (0.95–2.01)	0.09

MTV, metabolic tumor volume; SUV, standardized uptake value; TLG, total lesion glycolysis; GLCM, grey-level co-occurrence matrix; DFS, disease-free survival; OS, overall survival.

Table 6 Histology-specific univariate associations with disease-free survival for AC (N=33) and SCC (N=26) patients

Metric	AC (N=33, N_{events}=17)		SCC (N=26, N_{events}=14)	
	HR (95% CI)	P value	HR (95% CI)	P value
MTV	1.31 (0.90–1.90)	0.16	0.95 (0.56–1.60)	0.84
SUV_{max}	1.45 (0.92–2.28)	0.11	0.74 (0.43–1.26)	0.26
SUV_{peak}	1.48 (0.94–2.33)	0.09	0.73 (0.42–1.27)	0.27
SUV_{mean}	1.58 (1.02–2.44)	0.04	0.74 (0.43–1.27)	0.28
TLG	1.50 (1.01–2.22)	0.04	0.89 (0.51–1.55)	0.69
Homogeneity	1.08 (0.67–1.76)	0.75	1.83 (1.12–2.98)	0.02
Entropy-GLCM	0.80 (0.5–1.29)	0.36	0.56 (0.34–0.92)	0.02
Dissimilarity	0.88 (0.55–1.40)	0.58	2.16 (1.30–3.59)	0.003

MTV, metabolic tumor volume; SUV, standardized uptake value; TLG, total lesion glycolysis; GLCM, grey-level co-occurrence matrix; AC, adenocarcinoma; SCC, squamous cell carcinoma.

survival events did not allow for this analysis in relation to OS in this population. Quantitative imaging characteristics summarized by histology and scanner type are presented in *Table S3* and *Figure S2*.

Discussion

The standard of care for the treatment of early-stage NSCLC (stage I/II) is lobectomy and mediastinal lymph node dissection. Even after an R0 resection with pathologically negative lymph nodes, risk for recurrence is approximately 2% to 5% per year, with 5-year survival rates as low as 50% in patients with stage II disease (27). Both the 2009 International Association for the Study of Lung Cancer (IASLC) staging system and NCCN guidelines highlight ^{18}F-FDG PET/CT scanning as a diagnostic aid (28,29). However, current FDG PET/CT use is largely limited to qualitative review. Tumors, even of the same histology, often demonstrate variable and distinct imaging characteristics (30). This study aimed to determine if quantitative metrics, including texture-based metrics describing heterogeneity, in ^{18}F-FDG PET/CT imaging might enhance the clinical prediction of disease recurrence following surgical resection.

The extraction of quantitative features from PET data (Radiomics) allows for a more comprehensive analysis of

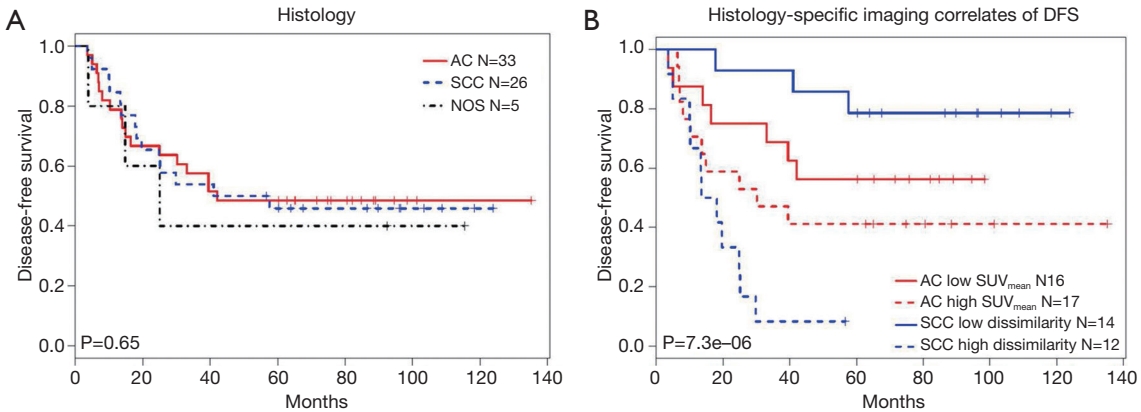

Figure 2 Kaplan-Meier survival analysis. (A) Histology was not shown to be a prognostic factor for 5-year disease-free survival. (B) Patients were classified into four separate groups based on histology and histology-specific correlates (Dissimilarity for SCC and SUV_{mean} for AC). Here, histology-specific median values reported in *Table 4* were used for dichotomizing patients into low (–) or high (+) groups. SCC, squamous cell carcinoma; SUV, standardized uptake value; AC, adenocarcinoma.

imaging characteristics that may be predictive of the biologic potential of a lung cancer (31,32). This assessment may be clinically relevant to define independent prognostic variables associated with survival in early-stage disease. Variable associations between texture features, including Entropy-GLCM and Dissimilarity, and treatment-related outcomes have been previously reported in NSCLC patients treated with SBRT (33,34). In our analysis, Entropy-GLCM was significantly associated with clinical endpoints in all patients, and was the only imaging metric to remain significant in a multivariate model of DFS and OS. Our results also demonstrate a significant association between imaging metrics and histology-specific DFS and OS.

In this study we demonstrate that histology specific differences in FDG heterogeneity may predict risk for recurrent disease. While differences in PET avidity between AC and SCC have been previously reported in both standard (8,10,11,35) and radiomics-based metrics (18,19). Their association with risk for recurrence was previously unknown. In this study, despite no significant differences in clinical endpoints, each histology showed unique imaging variables associated with DFS (*Figure 2*). Texture features, including Dissimilarity and Entropy-GLCM, were significant correlates of DFS in SCC patients. More commonly used SUV metrics describing tracer avidity, such as SUV_{mean}, demonstrated a moderately significant association with DFS. There is wide molecular variability observed within the AC histology (e.g., EGFR or ALK mutations), which may impact our quantitative analysis (36,37).

Established clinical metrics were significantly associated with DFS in this study. Pathological nodal status was the most predictive univariate variable for OS and 5-year DFS. However, pathological node status did not remain significantly independent in multivariate analysis. Other clinical metrics associated with survival in univariate and multivariate analyses included the use of adjuvant chemotherapy, pre-surgical hemoglobin, hypertension, and DLCO; all established clinical risk factors that impact survival (29). Within this study, no stage-specific differences of 5-year DFS were observed, likely due to the small number of patients. Commonly used FDG metric SUV_{max} was not strongly associated with OS, 5-year DFS, or risk for recurrence. These study conclusions are consistent with other modern series in which preoperative SUV_{max} is a poor independent prognostic factor due to its strong association with tumor size and stage (35,38).

There are several limitations that impact the translation of our study and require further validation. Foremost is the small sample size, which prevented extending our multivariate analysis to each histologic subtype and requires further exploration in a larger patient cohort matched for clinical characteristics and image acquisition across histologies. FDG texture features have been shown to be highly sensitive to reconstruction variation and MTV measurements (39,40). We have attempted to address these concerns by including robust and repeatable heterogeneity features characterized in prior work (24). Additionally, only

tumors with metabolic volumes >2 cm^3 were evaluated in this study to avoid sensitivity to very small tumor volumes, including lack of reproducible segmentations and texture extraction. Partial volume effects and respiratory motion were not addressed within this study. Future prospective studies that include harmonization of PET/CT scans from multiple institutions will allow for a broader application of these study conclusions.

Higher-order extraction of FDG PET/CT features show promise in evaluating associations between imaging characteristics and molecular drivers of disease. Linking these imaging features with tumor histology, stage, and potentially serum-based biomarkers may provide a platform for improved classification of early-stage NSCLC (41). This multifactorial diagnostic algorithm may be particularly helpful in identifying patient subsets at high risk for recurrence. This work motivates future studies to validate the role of quantitative FDG PET measures for predicting surgical outcomes in early-stage disease, where particular evaluation of histology-specific imaging signatures may be helpful to define high-risk patients.

Acknowledgements

Funding: Research reported in this publication was supported by the National Cancer Institute of the National Institutes of Health under Award Number T32CA009206. The content is solely the responsibility of the authors and does not necessarily represent the official views of the National Institutes of Health.

Footnote

Conflicts of Interest: The authors have no conflicts of interest to declare.

Ethical Statement: The Institutional Review Board at the University of Wisconsin approved this study including a waiver for patient consent due to the retrospective and de-identified nature of the data (IRB #2015-0266).

References

1. Malvezzi M, Bertuccio P, Levi F, et al. European cancer mortality predictions for the year 2014. Ann Oncol 2014;25:1650-6.
2. Hung JJ, Yeh YC, Jeng WJ, et al. Predictive Value of the International Association for the Study of Lung Cancer/American Thoracic Society/European Respiratory Society Classification of Lung Adenocarcinoma in Tumor Recurrence and Patient Survival. J Clin Oncol 2014;32:2357-64.
3. El-Sherif A, Gooding WE, Santos R, et al. Outcomes of sublobar resection versus lobectomy for stage I non-small cell lung cancer: a 13-year analysis. Ann Thorac Surg 2006;82:408-15; discussion 415-6.
4. Reich J, Asaph J. Natural history of stage I lung cancer. Chest 2007;132:2062; author reply 2062-3.
5. Berghmans T, Dusart M, Paesmans M, et al. Primary tumor standardized uptake value (SUVmax) measured on fluorodeoxyglucose positron emission tomography (FDG-PET) is of prognostic value for survival in non-small cell lung cancer (NSCLC): a systematic review and meta-analysis (MA) by the European Lung Cancer Working Party for the IASLC Lung Cancer Staging Project. J Thorac Oncol 2008;3:6-12.
6. Paesmans M, Berghmans T, Dusart M, et al. Primary tumor standardized uptake value measured on fluorodeoxyglucose positron emission tomography is of prognostic value for survival in non-small cell lung cancer: update of a systematic review and meta-analysis by the European Lung Cancer Working Party for the International Association for the Study of Lung Cancer Staging Project. J Thorac Oncol 2010;5:612-9.
7. Bazan JG, Duan F, Snyder BS, et al. Metabolic tumor volume predicts overall survival and local control in patients with stage III non-small cell lung cancer treated in ACRIN 6668/RTOG 0235. Eur J Nucl Med Mol Imaging 2017;44:17-24.
8. Agarwal M, Brahmanday G, Bajaj SK, et al. Revisiting the prognostic value of preoperative (18)F-fluoro-2-deoxyglucose ((18)F-FDG) positron emission tomography (PET) in early-stage (I & II) non-small cell lung cancers (NSCLC). Eur J Nucl Med Mol Imaging 2010;37:691-8.
9. Hyun SH, Choi JY, Kim K, et al. Volume-based parameters of (18)F-fluorodeoxyglucose positron emission tomography/computed tomography improve outcome prediction in early-stage non-small cell lung cancer after surgical resection. Ann Surg 2013;257:364-70.
10. Jeong HJ, Min JJ, Park JM, et al. Determination of the prognostic value of [(18)F]fluorodeoxyglucose uptake by using positron emission tomography in patients with non-small cell lung cancer. Nucl Med Commun 2002;23:865-70.
11. Downey RJ, Akhurst T, Gonen M, et al. Preoperative

F-18 fluorodeoxyglucose-positron emission tomography maximal standardized uptake value predicts survival after lung cancer resection. J Clin Oncol 2004;22:3255-60.
12. Mangili F, Cigala C, Arrigoni G, et al. Cell loss and proliferation in non-small cell lung carcinoma: correlation with histological subtype. Eur J Histochem 1998;42:287-95.
13. El Naqa I, Grigsby P, Apte A, et al. Exploring feature-based approaches in PET images for predicting cancer treatment outcomes. Pattern Recognit 2009;42:1162-71.
14. Hatt M, Visvikis D, Albarghach NM, et al. Prognostic value of 18F-FDG PET image-based parameters in oesophageal cancer and impact of tumour delineation methodology. Eur J Nucl Med Mol Imaging 2011;38:1191-202.
15. Miles KA, Ganeshan B, Griffiths MR, et al. Colorectal cancer: texture analysis of portal phase hepatic CT images as a potential marker of survival. Radiology 2009;250:444-52.
16. Nakajo M, Jinguji M, Shinaji T, et al. A Pilot Study of Texture Analysis of Primary Tumor [18F]FDG Uptake to Predict Recurrence in Surgically Treated Patients with Non-small Cell Lung Cancer. Mol Imaging Biol 2018. [Epub ahead of print].
17. Han S, Woo S, Suh CH, et al. A systematic review of the prognostic value of texture analysis in. Ann Nucl Med 2018;32:602-10.
18. Orlhac F, Soussan M, Chouahnia K, et al. 18F-FDG PET-Derived Textural Indices Reflect Tissue-Specific Uptake Pattern in Non-Small Cell Lung Cancer. PLoS One 2015;10:e0145063.
19. Ha S, Choi H, Cheon GJ, et al. Autoclustering of Non-small Cell Lung Carcinoma Subtypes on (18)F-FDG PET Using Texture Analysis: A Preliminary Result. Nucl Med Mol Imaging 2014;48:278-86.
20. Wahl RL, Jacene H, Kasamon Y, et al. From RECIST to PERCIST: Evolving Considerations for PET response criteria in solid tumors. J Nucl Med 2009;50 Suppl 1:122S-50S.
21. Galavis PE, Paliwal B, Holden J, et al. System and method for gradient assisted non-connected automatic region (GANAR) analysis. Google Patents, 2016.
22. Haralick RM, Shanmugam K, Dinstein I. Textural features for image classification. IEEE Trans Syst Man Cybernet 1973;SMC-3:610-21.
23. Tang X. Texture information in run-length matrices. IEEE Trans Image Process 1998;7:1602-9.
24. Galavis PE, Hollensen C, Jallow N, et al. Variability of textural features in FDG PET images due to different acquisition modes and reconstruction parameters. Acta Oncol 2010;49:1012-6.
25. Galavis PE. Robust tumor segmentation for radiotherapy target definition. Madison, WI: University of Wisconsin, Madison, 2013.
26. Maani R, Yang YH, Kalra S. Voxel-based texture analysis of the brain. PLoS One 2015;10:e0117759.
27. Jemal A, Murray T, Ward E, et al. Cancer statistics, 2005. CA Cancer J Clin 2005;55:10-30.
28. Mountain CF. A new international staging system for lung cancer. 1986. Chest 2009;136:e25.
29. Ettinger DS, Akerley W, Borghaei H, et al. Non-small cell lung cancer, version 2.2013. J Natl Compr Canc Netw 2013;11:645-53; quiz 653.
30. Rees JH, Smirniotopoulos JG, Jones RV, et al. Glioblastoma multiforme: radiologic-pathologic correlation. Radiographics 1996;16:1413-38; quiz 1462-3.
31. Lambin P, Rios-Velazquez E, Leijenaar R, et al. Radiomics: extracting more information from medical images using advanced feature analysis. Eur J Cancer 2012;48:441-6.
32. Kumar V, Gu Y, Basu S, et al. Radiomics: the process and the challenges. Magn Reson Imaging 2012;30:1234-48.
33. Pyka T, Bundschuh RA, Andratschke N, et al. Textural features in pre-treatment [F18]-FDG-PET/CT are correlated with risk of local recurrence and disease-specific survival in early stage NSCLC patients receiving primary stereotactic radiation therapy. Radiat Oncol 2015;10:100.
34. Lovinfosse P, Janvary ZL, Coucke P, et al. FDG PET/CT texture analysis for predicting the outcome of lung cancer treated by stereotactic body radiation therapy. Eur J Nucl Med Mol Imaging 2016;43:1453-60.
35. Vesselle H, Turcotte E, Wiens L, et al. Relationship between non-small cell lung cancer fluorodeoxyglucose uptake at positron emission tomography and surgical stage with relevance to patient prognosis. Clin Cancer Res 2004;10:4709-16.
36. Choi H, Paeng JC, Kim DW, et al. Metabolic and metastatic characteristics of ALK-rearranged lung adenocarcinoma on FDG PET/CT. Lung Cancer 2013;79:242-7.
37. Yip SS, Kim J, Coroller T, et al. Associations between somatic mutations and metabolic imaging phenotypes in non-small cell lung cancer. J Nucl Med 2017;58:569-76.
38. Vesselle H, Freeman JD, Wiens L, et al. Fluorodeoxyglucose uptake of primary non-small cell lung cancer at positron emission tomography: new contrary data on prognostic role. Clin Cancer Res 2007;13:3255-63.
39. Brooks FJ, Grigsby PW. The effect of small tumor volumes on studies of intratumoral heterogeneity of tracer

uptake. J Nucl Med 2014;55:37-42.
40. Traverso A, Wee L, Dekker A, et al. Repeatability and Reproducibility of Radiomic Features: A Systematic Review. Int J Radiat Oncol Biol Phys 2018;102:1143-58.
41. Rinewalt D, Shersher DD, Daly S, et al. Development of a serum biomarker panel predicting recurrence in stage I non-small cell lung cancer patients. J Thorac Cardiovasc Surg 2012;144:1344-50; discussion 1350-1.

Cite this article as: Harmon S, Seder CW, Chen S, Traynor A, Jeraj R, Blasberg JD. Quantitative FDG PET/CT may help risk-stratify early-stage non-small cell lung cancer patients at risk for recurrence following anatomic resection. J Thorac Dis 2019;11(4):1106-1116. doi: 10.21037/jtd.2019.04.46

Supplementary

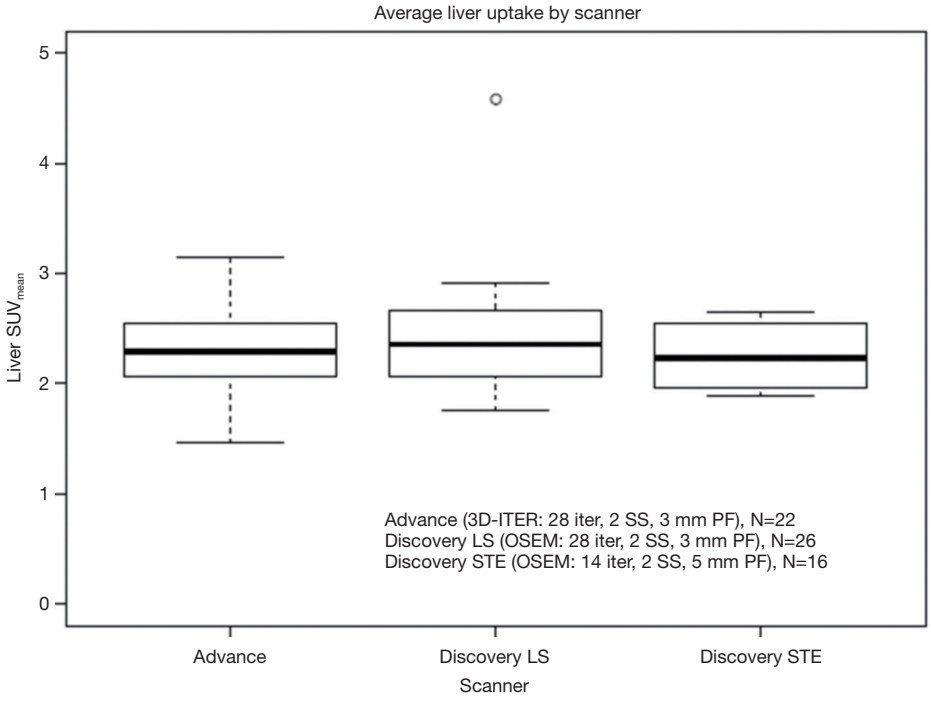

Figure S1 Average liver uptake for each patient, calculated from a 3 cm diameter sphere. Patients were separated by which scanner their FDG PET/CT was acquired on, no significant differences in uptake patterns were noted.

Table S1 Imaging correlation with tumor size from pathology (pathological size) and imaging (MTV)

Metric	Path. size		MTV	
	ρ	P value	ρ	P value
MTV	0.85	<0.001	–	–
SUV_{max}	0.61	<0.001	0.59	<0.0001
SUV_{peak}	0.63	<0.001	0.62	<0.0001
SUV_{mean}	0.55	<0.001	0.53	<0.0001
TLG	0.85	<0.001	0.94	<0.0001
Homogeneity	–0.29	0.01	–0.38	0.002
Entropy-GLCM	0.32	0.01	0.4	0.001
Dissimilarity	–0.36	0.004	–0.38	0.002

SUV, standardized uptake value; TLG, total lesion glycolysis; GLCM, grey-level co-occurrence matrix.

Table S2 Final multivariate model after backwards selection using BIC criteria. Variables considered: clinical stage, smoking status, tumor grade, mediastinal staging, pathologic node status, hemoglobin levels, DLCO, history of hypertension, use of adjuvant chemotherapy, SUV_{max}, SUV_{peak}, SUV_{mean}, Homogeneity, Entropy-GLCM

Metric	DFS (N_{events}=34)		OS (N_{events}=26)	
	HR (95% CI)	P value	HR (95% CI)	P value
Hemoglobin	0.76 (0.61–0.94)	0.01		
DLCO	0.95 (0.93–0.98)	0.005	0.96 (0.94–0.99)	0.005
Hypertension	2.83 (1.29–6.22)	0.01	2.97 (1.17–7.52)	0.02
Tumor grade (mod/poor)	8.9 (1.9–41)	0.005		
Entropy-GLCM	0.65 (0.49–0.87)	0.004	0.60 (0.45–0.81)	0.0007
Adjuvant chemotherapy	1.19 (0.87–1.64)	0.28	4.79 (1.9–12)	0.09

DLCO, diffusing capacity of the lungs for carbon monoxide; GLCM, grey-level co-occurrence matrix.

Table S3 Histologic summary by scanner type, with DFS and OS events reported as (# DFS events/# OS events)

Scanner	AC	SCC	Other
Advance	12 (5/5)	7 (2/1)	3 (1/0)
Dis LS	16 (9/8)	8 (4/3)	2 (2/1)
Dis STE	5 (3/2)	11 (8/6)	0

AC, adenocarcinoma; SCC, squamous cell carcinoma; DFS, disease-free survival; OS, overall survival.

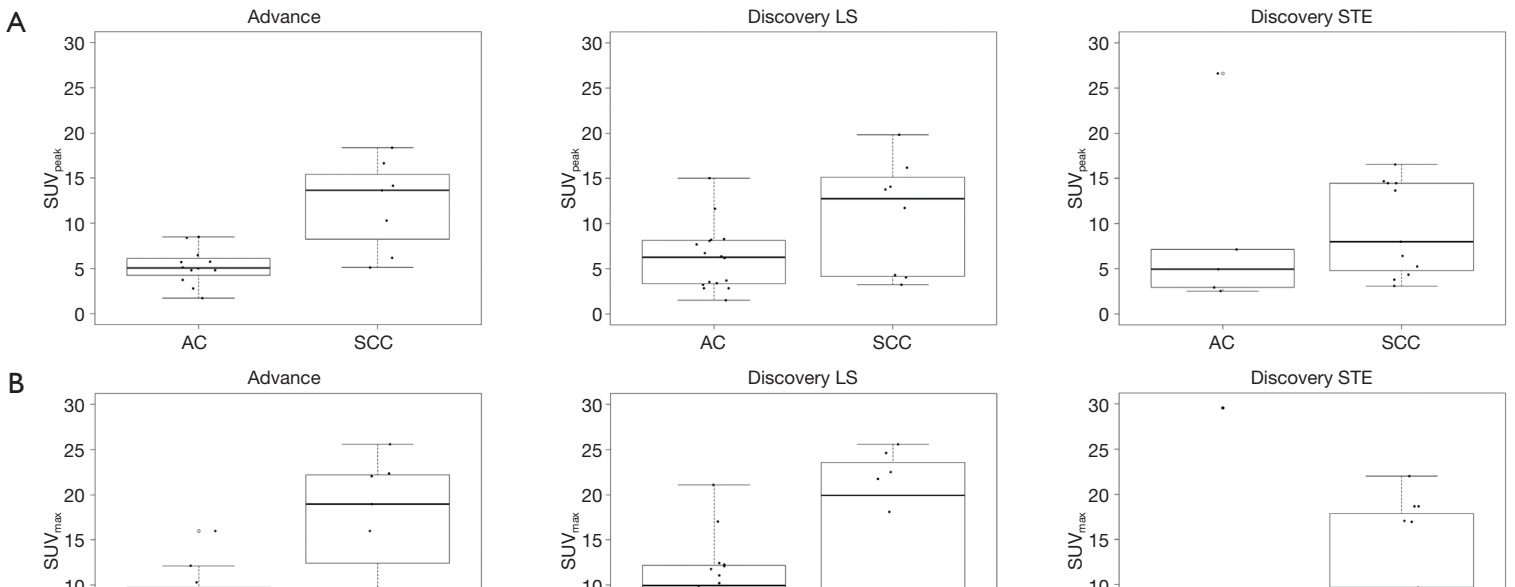

Figure S2 Imaging metrics *vs.* histology for each scanner model: (A) SUV_{peak}, (B) SUV_{max}, (C) SUV_{mean}, (D) Homogeneity, (E) Entropy-GLCM, (F) Dissimilarity.